MODELLING OF HELIUM SPECTRUM IN SOLAR PROMINENCES

N. Labrosse, P. Gouttebroze

Institut d'Astrophysique Spatiale, Université Paris XI/CNRS, Bat. 121, 91405 Orsay Cedex, France
labrosse@ias.fr, gouttebroze@ias.fr

ABSTRACT

We present non-LTE calculations for the neutral and ionized helium spectrum in quiescent solar prominences. The hydrogen and helium atoms are multilevel model atoms, including for helium the three stages of ionization. Departures from Local Thermodynamic Equilibrium are allowed for each level. We investigate the formation of lines and continuum within the frame of one dimensional, isothermal and isobaric static slab models. The numerical code used for these calculations allows also the study of Partial Redistribution effects for several lines. In the present work we show the effects of three free parameters which are the electron temperature, the gas pressure, and the slab width. Those preliminary results will be compared in a future work with former theoretical computations and we will use this numerical code as a diagnostic tool to analyze helium lines observations.

Key words: helium:lines; Sun:prominences.

1. INTRODUCTION

Observations of solar helium lines become frequent nowadays, especially with SoHO instruments for the EUV part of the solar helium spectrum. The Coronal Diagnostic Spectrometer, the Extreme Ultraviolet Imaging Telescope and the Solar Ultraviolet Measurement of Emitted Radiation which are on board of the Solar Heliospheric Observatory provide us a large amount of observations that need powerful diagnostic tools to give accurate physical parameters as the temperature, the gas pressure, or the population densities. Some spectral observations in different spectral ranges can also be made from ground based observatories. In order to allow such diagnostics we use two different numerical codes. HYDR computes the hydrogen spectrum and determines the electron density (Gouttebroze et al. 1993, hereafter GHV). A new version of SIMPLI has been written to calculate the helium lines, from an earlier version used for calcium lines (Gouttebroze et al. 1997). In the following we present preliminary results for new computations of He I and He II lines emitted by irradiated prominences for a set of different prominence models similar to those of GHV and the dependence of emerging spectrum on temperature, pressure, and prominence slab width.

2. COMPUTATIONS

2.1. Prominence Model

Our model consists of plane-parallel slabs standing vertically above the solar surface. Observations are made in a direction perpendicular to the slab surface (Figure 1). The prominence is illuminated on both surfaces by an incident radiation field which determines the boundary conditions for the resolution of the radiative transfer equations. This radiation field comes from the photosphere, the chromosphere and the corona and is deduced from observations of the solar disk. The models are defined by the temperature, the gas pressure, the microturbulent velocity and the thickness of the slab. The first three quantities are supposed to be constant throughout the slab. In this work we present some results for a subset of 13 models of the GHV grid: 5 temperatures (4300, 6000, 8000, 10000, and 15000 K), 5 gas pressures (0.02, 0.05, 0.1, 0.2, 0.5 dyn cm^{-2}), and 5 slab width (200, 500, 1000, 2000, and 5000 km). In all these models the microturbulent velocity is set to 5 km s^{-1}.

2.2. The Model Atom

For the hydrogen atom, we use a 20 bound levels plus continuum atom (see GHV for more details). For the helium atom, we use 13 bound levels for neutral helium, 2 bound levels for the first ionization stage, and finally the continuum. Thus we can obtain for He I 3 resonance lines and 19 subordinate lines, and 1 He II resonance line. The helium resonance lines stand all in the EUV part of the solar spectrum and can only be observed by space observatories. Table 1 summarizes some of the atomic data used here.

2.3. Numerical Procedure

The computations are first made for hydrogen to obtain the hydrogen spectrum, the level populations, the electron densities and the mean intensities at

Proceedings 8th SOHO Workshop 'Plasma Dynamics and Diagnostics in the Solar Transition Region and Corona', Paris, France, 22-25 June 1999, (ESA SP-446, October 1999)

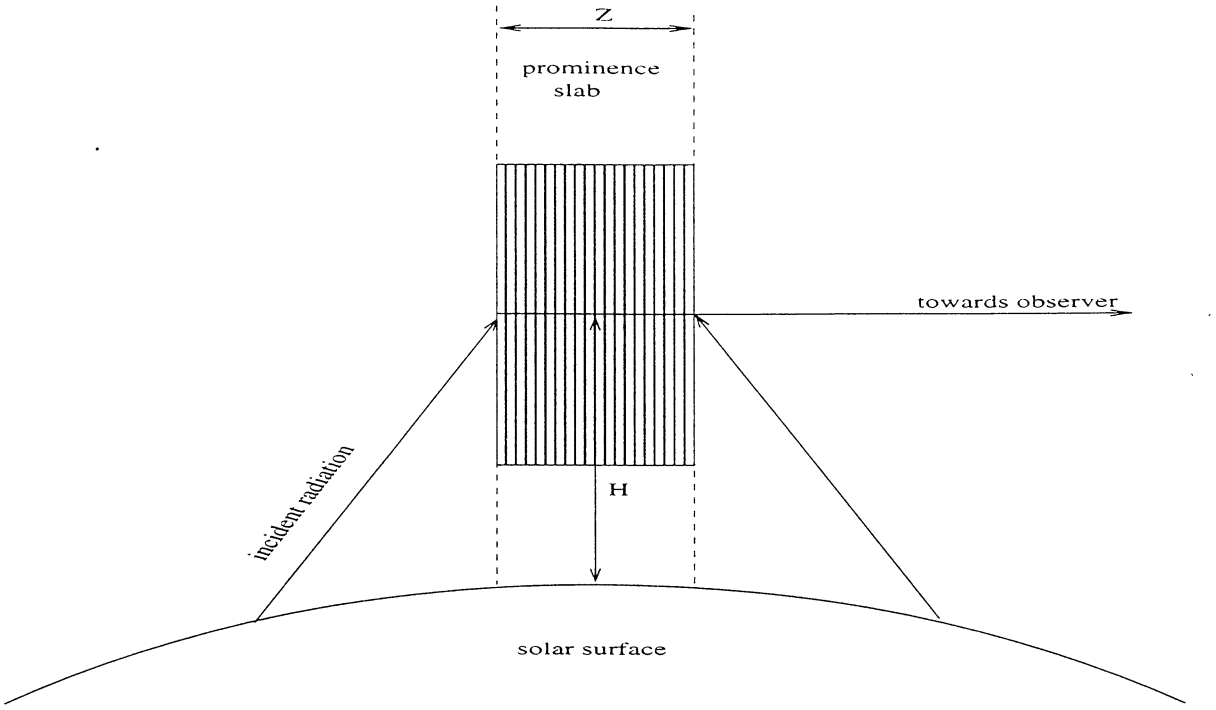

Figure 1. Model of irradiated prominence.

different wavelengths for different depths inside the slab. The statistical equilibrium equations of hydrogen atoms are solved by iteration. The radiative transfer equations in optically thick transitions are solved by the Feautrier method with variable Eddington factors. The incident intensities are deduced from observations of the solar disk. Then the same equations are solved for helium with the incident radiation field in helium lines wavelengths from Heasley et al. 1974, and taking into account the radiation field in the slab due to hydrogen. The resonance lines are treated in partial frequency redistribution.

3. HELIUM IONIZATION

We study here the He II / He I population ratio in the slab for different models showing the effect of electron temperature, gas pressure and slab thickness. Figure 2 presents the variations of this ratio across the slab, each panel corresponding to the study of one free parameter effect.
For thin slabs the ratio is larger than for thick slabs, and He II is still important in the center of thin slabs. The total helium population is nearly constant at the surface of the slab but increases with thickness in the slab center. At the temperature of 8000 K, the main part of helium is in the ground state of He I.
At high temperature the He II / He I population ratio is larger than at lower temperatures. At the slab surface the effect of incident radiation for high temperatures models yields helium ionization. When we are going deeper in the slab helium atoms are less sensitive to incident radiation and if we increase the temperature the particle density decreases.
The number of helium atoms increases with pressure and since the temperature of 8000 K is not sufficient to ionize helium efficiently, almost all particles are in neutral stage.

4. EMERGENT LINE PROFILES AND INTEGRATED INTENSITIES

We present emergent half profiles (for an observation angle μ=cos θ=1) and integrated intensities plots for four often observed lines: the He I $\lambda\lambda$ 10830, 584, and 5876 (D3) Å and He II λ 304 Å lines. The He I $\lambda\lambda$ 10830 and 5876 Å are optically thin lines, and the He I λ 584 Å and He II λ 304 Å are two optically thick resonance lines. Figure 3, 4, and 5 show respectively the effect on emergent line profile and integrated intensities of varying the slab width, the temperature and the pressure.
For the optically thin lines the integrated intensity increases with slab thickness (figure 3). For high thicknesses (above 1000 km) the variations for line center intensity and line width are less important. The optically thick lines are saturated and the pressure variations have no effect.
We can see clearly on figure 4 that at low temperatures (up to 10000 K) there is only scattering of incident radiation in the line cores, the effect of the temperature increase being an increase in line width. Note the saturation of the He I λ 584 Å line core. At high temperature collisions effects become important and result in a sharp increase in the integrated intensity. This is obvious on the lines profiles: the

Table 1. Helium energy levels and line transitions. In lower table bold caracters indicate resonance lines.

Level	Ion	Spectr. term	Excitation frequency (x 10^{15} Hz)	Statistical weight
1	He I	1s ^{1}S	0.0	1
2		2s ^{3}S	4.792364	3
3		2s ^{1}S	4.984880	1
4		2p ^3P	5.069096	9
5		2p ^{1}P	5.130510	3
6		3s ^{3}S	5.493312	3
7		3s ^{1}S	5.542120	1
8		3p ^{3}P	5.563100	9
9		3d ^{3}D	5.579195	15
10		3d ^1D	5.579508	5
11		3p ^{1}P	5.582430	3
12		4s ^{3}S	5.738150	48
13		4s ^{1}S	5.738610	16
14	He II	n=1	5.948600	2
15		n=2	15.81100	8
16	He III	...	19.10900	1

i-level	j-level	λ (Å)	Einstein coefficient	i-level	j-level	λ (Å)	Einstein coefficient
2	4	10 830	1.02 10^7	2	12	3 170	9.5 10^5
1	**5**	**584**	**1.8 10^9**	4	12	4 481	8.5 10^6
3	5	20 590	1.98 10^6	8	12	17130	2.5 10^6
4	6	7 067	2.78 10^7	9	12	18 860	6.2 10^6
5	7	7 283	1.81 10^7	**1**	**13**	**522**	**4.6 10^7**
2	8	3 890	9.48 10^6	3	13	3 977	1.34 10^6
6	8	42 960	1.08 10^6	5	13	4 930	6.72 10^6
4	9	5 877	7.06 10^7	7	13	15 260	2.6 10^5
5	10	6 677	6.36 10^7	10	13	18 840	6.09 10^6
1	**11**	**537**	**5.66 10^8**	11	13	19 200	2.5 10^6
3	11	5 017	1.33 10^7				
7	11	74370	2.53 10^5	**14**	**15**	**304**	**7.51 10^9**

emission at optically thin line center is much more important than at low temperatures, and the wings are much larger. For the He I resonance line there is a reversal at line center due to very high opacity at 15000 K and an emission peak in the wing at optical depth unity. For the He II resonance line there is scattering of incident radiation at low temperatures and self emission above 10000 K. Both resonance lines have decreasing optical depth with temperature.
For optically thin lines the pressure increase generates a decrease in the integrated intensities, fainter line center and wings, and smaller line widths (figure 5), the optical depths also decrease. For the first He I resonance line, there is no variation in emerging spectrum, but its optical depth increases with gas pressure. The He II resonance line optical depth decreases with pressure and thus the line center intensity, the wing intensity, and the line width are decreasing. This is due to a sharp decrease of He II population in the center of the slab while at the surface the He II population increases slowly with pressure.

5. CONCLUSIONS

This preliminary work allows us to study the general behaviour of the helium spectrum in solar quiescent prominences for a large number of models including a broad range of temperatures, pressures, and slab widths which correspond to usually observed physical quantities for prominences. We have shown how those physical parameters can influence helium ionization and emitted intensities. Therefore we have now to compare these results with former simulations done by Heasley and Milkey (Heasley & Milkey 1976, Heasley & Milkey 1978, Heasley & Milkey 1983), and try to correlate them with hydrogen observations. Then a comparison with SoHO observations of quiescent prominences could be done, particularly using the He I λ 584 Å and He II λ 304 Å observations made by CDS. SUMER and EIT. We should also increase the number of He II levels to reproduce more ionized helium lines since some of them are observed (e.g., Laming & Feldman 1993). This will be the subject of a future work.

ACKNOWLEDGEMENTS

We thank Eugene Avrett for providing us with atomic data for neutral helium (from ion model He1L13).
Computations were performed using the facilities of the 'Institut du Développement des Ressources en In-

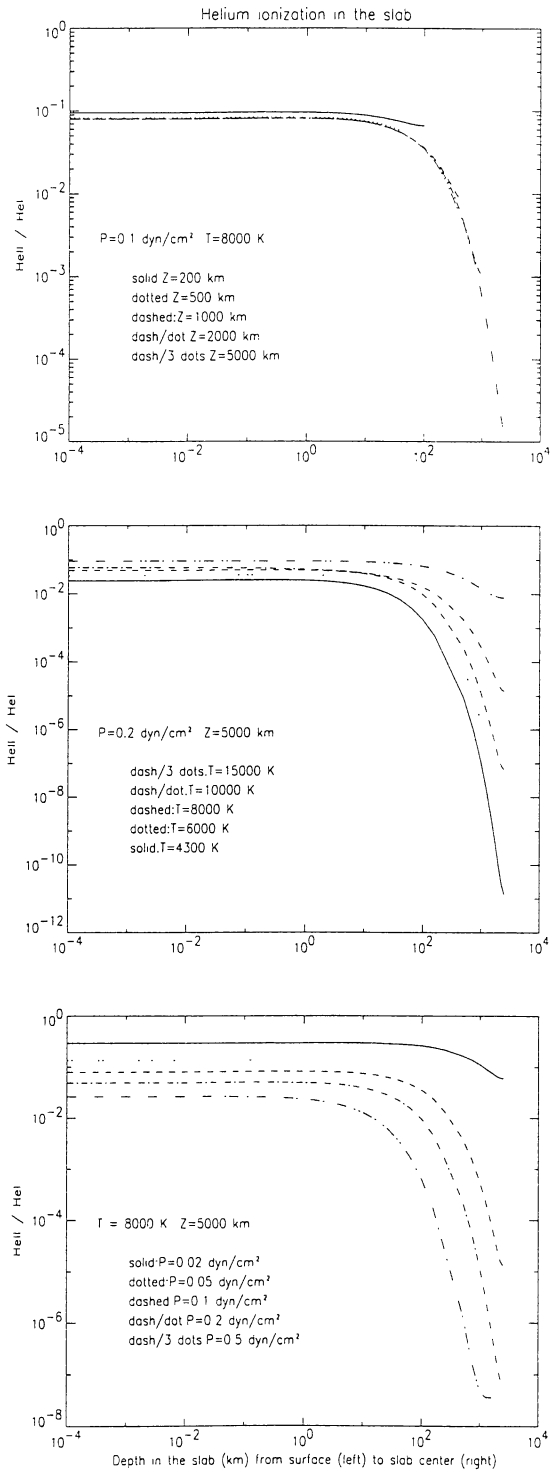

Figure 2. n(HeII)/n(HeI) vs depth in the slab for different models. From top to bottom: effect of slab thickness, of temperature, and of gas pressure.

formatique Scientifique' (IDRIS, Orsay).

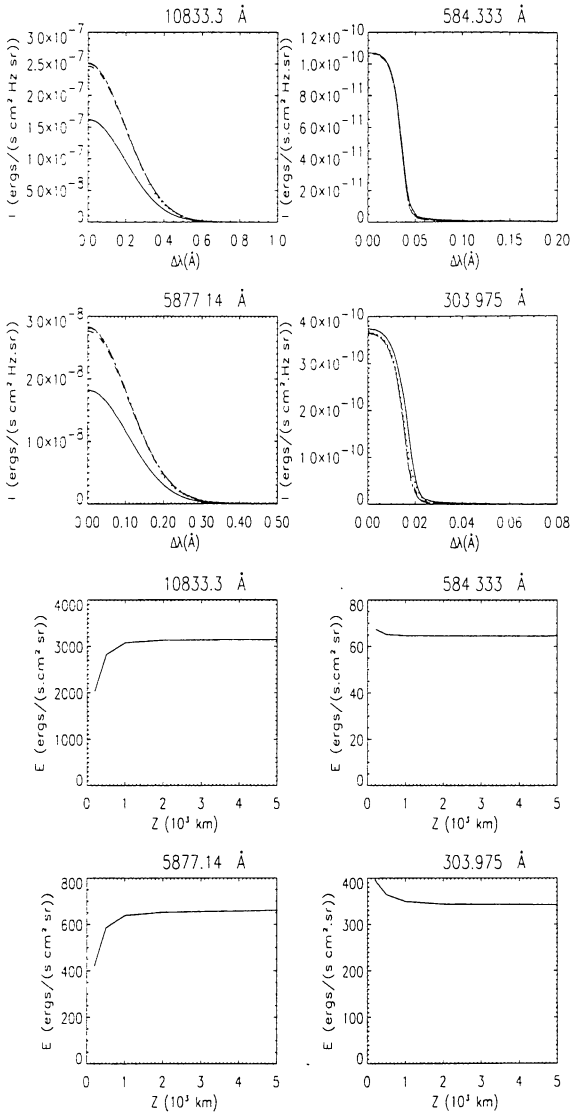

Figure 3. Half profiles of emergent intensity and integrated intensities variations with slab thickness (T=8000 K, P=0.1 dyn cm^{-2}). Four top panels: Z=200 (solid line), Z=500 (dotted), Z=1000 (dashed), Z=2000 (dash/dot), Z=5000 km (dash/3 dots).

REFERENCES

Gouttebroze, P., Heinzel, P., Vial, J.-C., 1993, Astron. Astrophys. Suppl., 99, 513

Gouttebroze, P., Vial, J.-C, Heinzel, P., 1997, Solar Physics, 172, 125

Heasley J.N., Mihalas D., Poland A.I., 1974, ApJ, 192, 181

Heasley J.N., Milkey R.W., 1976, ApJ, 210, 827

Heasley J.N., Milkey R.W., 1978, ApJ, 221, 677

Heasley J.N., Milkey R.W., 1983, ApJ, 268, 398

Laming, J.M., Feldman U., 1993, ApJ, 403, 434

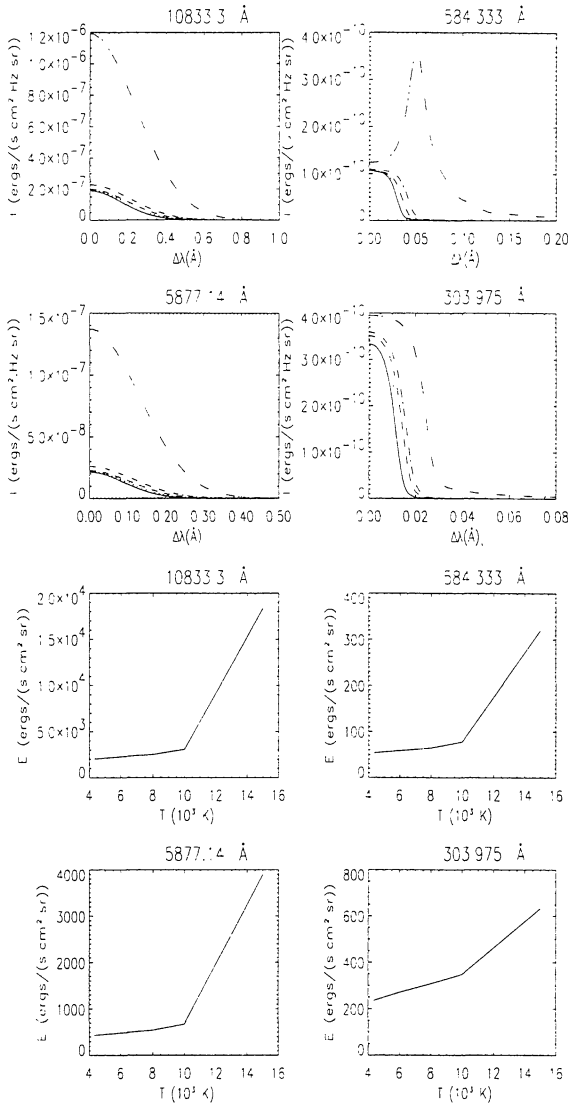

Figure 4. Half profiles of emergent intensity and integrated intensities variations with electron temperature (P=0.2 dyn cm^{-2}, Z=5000 km). Four top panels: T=4300 (solid line), T=6000 (dotted), T=8000 (dashed), T=10000 (dash/dot), T=15000 K (dash/3 dots).

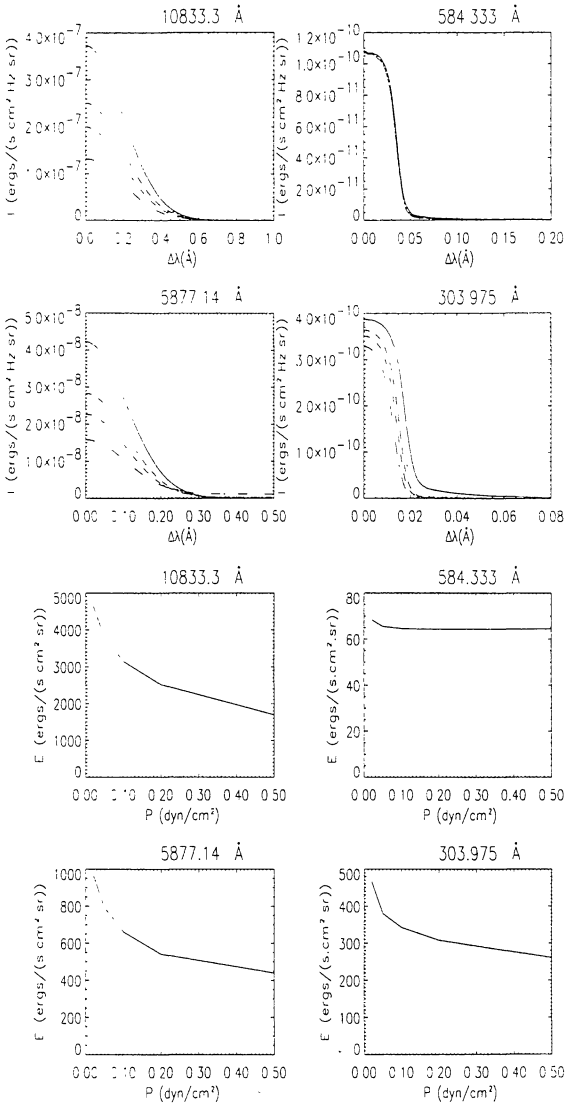

Figure 5. Half profiles of emergent intensity and integrated intensities variations with gas pressure (T=8000 K, Z=5000 km). Four top panels: P=0.02 (solid line), P=0.05 (dotted), P=0.1 (dashed), P=0.2 (dash/dot), P=0.5 dyn cm^{-2} (dash/3 dots).